Electronic Supplementary Material (ESI) for RSC Advances.

Supporting Information (SI) for

Two nitrogen-rich Ni (II) coordination compounds based on 5,5'-azotetrazole: Synthesis, characterization and effect on thermal decomposition for RDX, HMX and AP

Dong Chen, Shiliang Huang, Qi Zhang, Qian Yu, Xiaoqing Zhou, Hongzhen Li* and Jinshan Li**

Institute of Chemical Materials, China Academy of Engineering Physics, Mianyang 621900, China.

*Address for correspondence. Email: jackzhang531@gmail.com

Phone: 86-816-2493145; Fax: 86-816-2485072

Table S1. Hydrogen bond distances and angles for $[Ni(en)_3]AZT \cdot THF$ (**1**)

D-H...A	d(D-H)(Å)	d(H...A)(Å)	d(D...A)(Å)	D-H...A(°)
N(14)-H(3A)···N(3)	0.919	2.126	3.053(6)	162.87
N(15)-H(5B)···N(5)	0.921	2.197	3.073(6)	158.58
C(16)-H(4B)···N(4)	0.920	2.225	3.096(6)	157.69

Table S2. Hydrogen bond distances and angles for $[Ni(AZT)(pn)_2]_n$ (**2**)

D-H···A	d(D-H)(Å)	d(H...A)(Å)	d(D...A)(Å)	D-H...A(°)
N(1)-H(1B)···N(6)	0.900	2.948	3.223	137.93

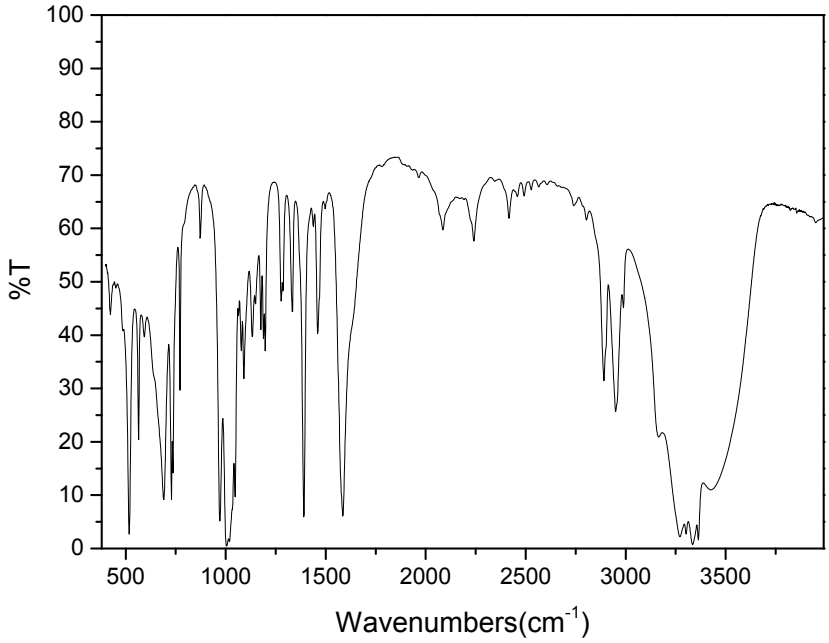

Fig. S1 The infrared spectrum of compound **1**

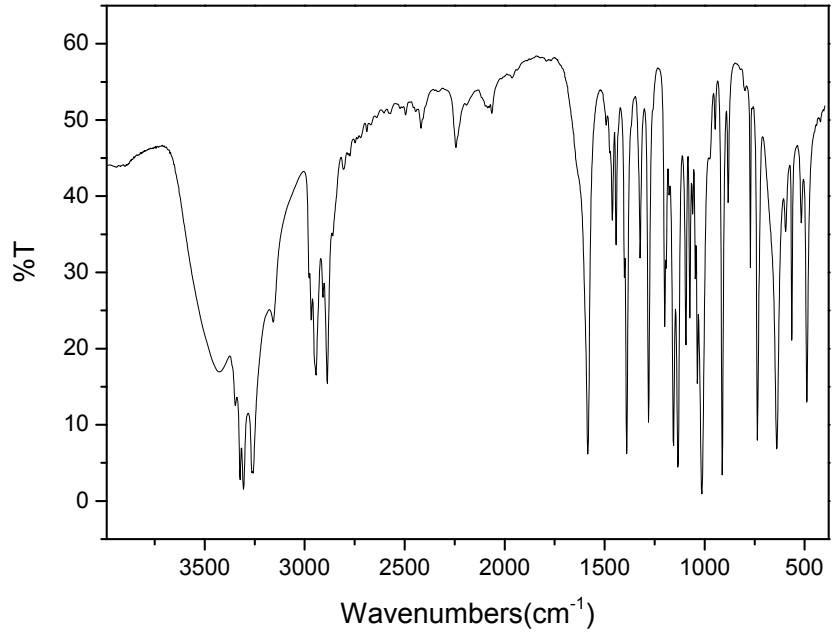

Fig. S2 The infrared spectrum of compound **2**

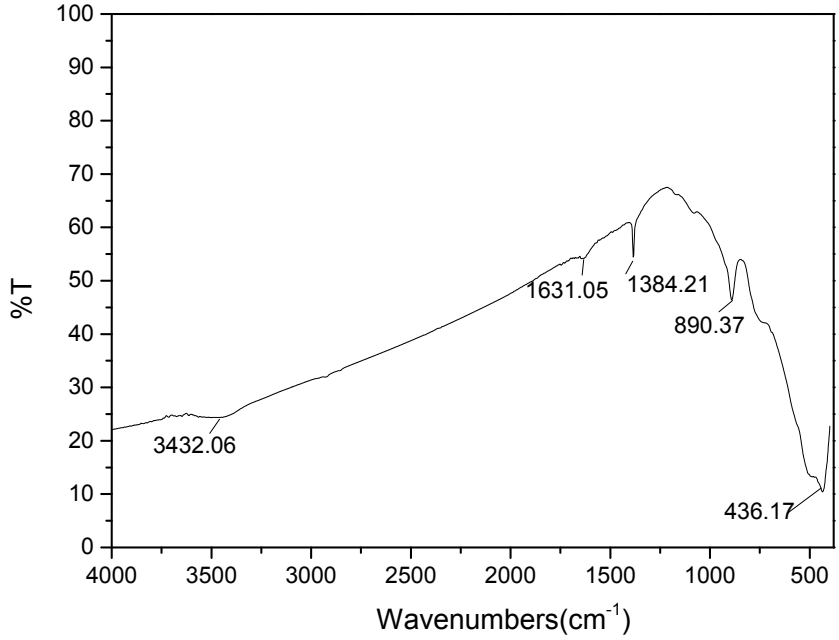

Fig. S3 The infrared spectrum of the final decomposed residues of **1** and **2** at 700 ℃

In Fig. S1-3, The characteristic absorption bands of $[Ni(en)_3]AZT \cdot THF$ **1** and $[Ni(AZT)(pn)_2]_n$ **2** have disappeared, the existence of the absorption peak around 436 cm^{-1} in both residues proves the final decomposed residue is mainly NiO.

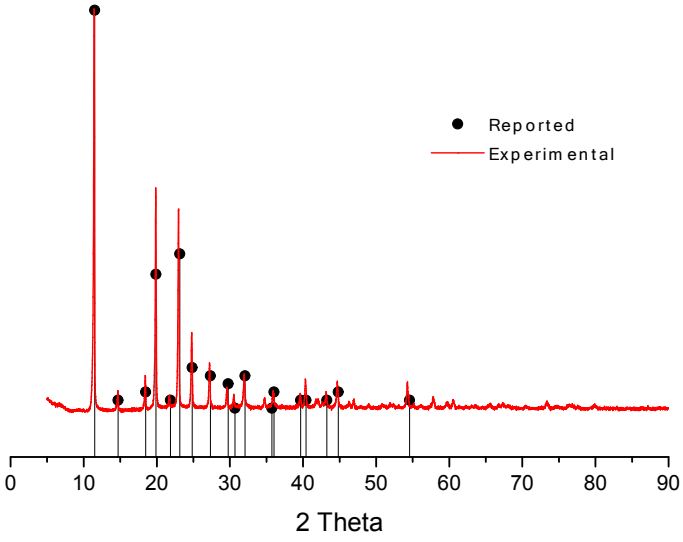

Fig. S4 XRPD diagrams for complex $Ni(en)_3SO_4$.

In Fig. S4, XRPD diagrams of the reported (PDF#23-1796) and experimental complex $Ni(en)_3SO_4$ were showed in Fig. 2, their main 2 Theta peaks are consistent, which means that they are the same compound.

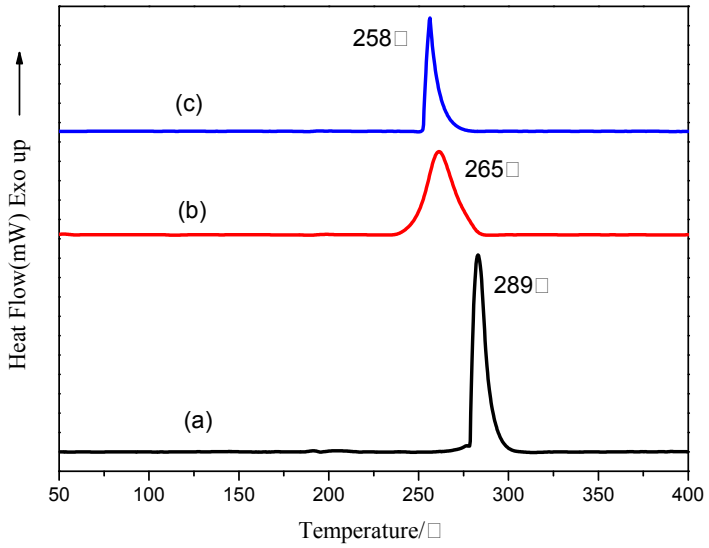

Fig. S5 DSC curves for HMX (a), SAZT+HMX (b) and $Ni(en)_3SO_4$+HMX (c).

The DSC curves of HMX and the mixtures of HMX with SAZT or $Ni(en)_3SO_4$ can be seen in Fig. S5. The only exothermic peak at 289 ℃ is due to the complete decomposition of HMX with the heat of 1279.5 J/g. From Fig. S5, we can see that the peak temperature of c (258 ℃) and b (265 ℃) is lower than that of pure HMX while

there decomposition heat has decreased to 600.58 J/g and 1113.29 J/g respectively. The sharp exothermic peak of c indicates a rapid decomposition process. We can see the decomposition temperature of c is much lower than b but b holds much more decomposition heat than c.

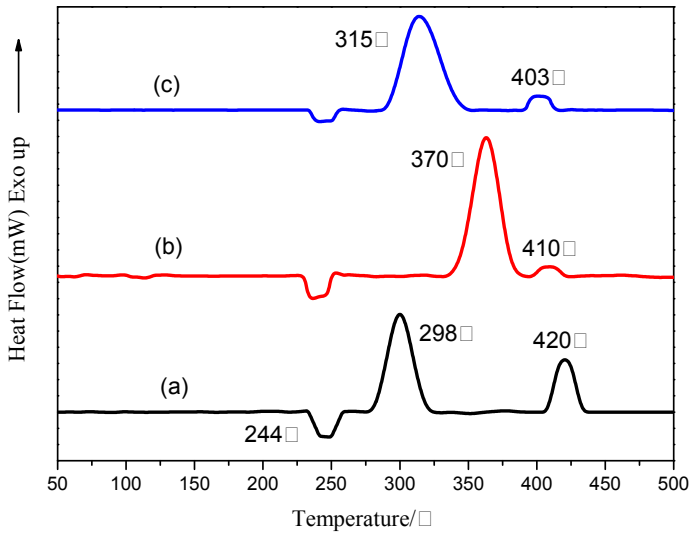

Fig. S6 DSC curves for AP (a), SAZT+AP (b) and $Ni(en)_3SO_4$+AP (c).

As is shown in Fig. S6, the DSC curves of AP and the mixtures of AP with SAZT or $Ni(en)_3SO_4$ are explored. There are two exothermic peaks of AP in Fig. 4a at 298 ℃ and 420 ℃, corresponding to the heat of 206.1 J/g and 133 J/g respectively in our tests. From Fig. S6b and c, we can see that the compounds have no significant impact on the phase transition, but there are some significant changes in the decomposition patterns. There is a main exothermic peak at 370 ℃ for b and 315 ℃ for c, corresponding to the heat of 299.68 J/g and 220.3 J/g respectively. It is apparent that the second exothermic peaks temperature of b (410 ℃) and c (403 ℃) are lower than that of pure AP (420 ℃). In terms of the main exothermic process, the decomposition temperature of c is much lower than b but b holds much more decomposition heat than c.

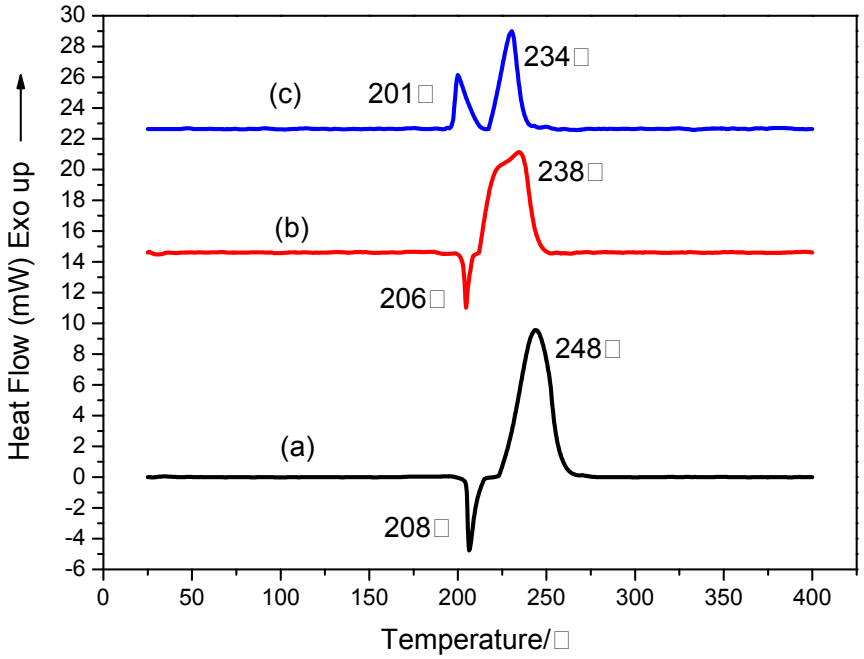

Fig. S7 DSC curves for RDX (a), 15%**1**+RDX (b) and 15%**2**+RDX (c).

Fig. S7 shows the DSC curves of RDX and the mixtures of RDX with compounds 15% **1** or 15% **2**. We can see that the melt peak of c has disappeared and there are two detached exothermic peaks instead. The main exothermic peaks temperature of b (238 ℃) and c (234 ℃) is a little lower than that of pure RDX (248 ℃), meanwhile the decomposition heat is 454 J/g for c and 1138 J/g for b.

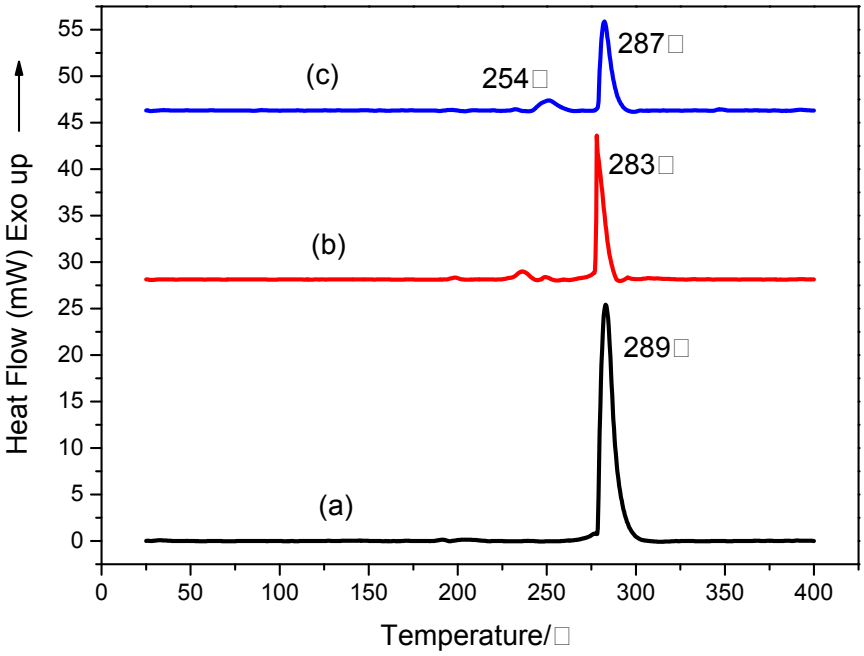

Fig. S8 DSC curves for HMX (a),15% **1**+HMX (b) and 15%**2**+HMX (c).

Fig. S8 shows the DSC curves of HMX and the mixtures of HMX with compounds 15% **1** or 15% **2**. We can see that the main exothermic peaks temperature of b (283 ℃) and c (287 ℃) is a little lower than that of pure HMX (298 ℃), and the decomposition heat is 422 J/g for c and 553 J/g for b.

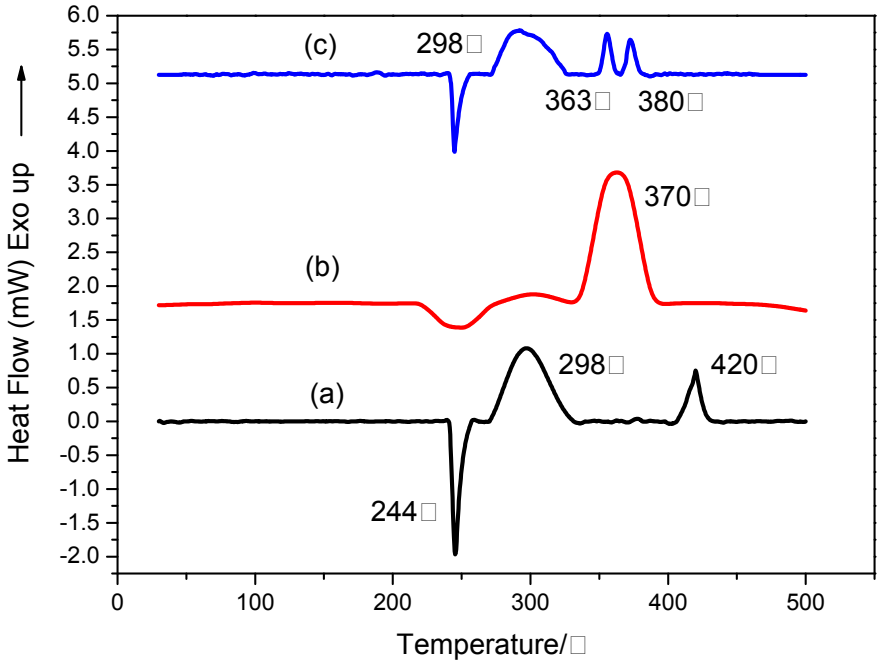

Fig. S9 DSC curves for AP (a), 15%**1**+AP (b) and 15%**2**+AP (c).

Fig. S9 shows the DSC curves of AP and the mixtures of AP with compounds 15% **1** or 15% **2**. We can see that the melt peaks of b and c have not changed. The first exothermic peak of b is disappeared and there are two detached exothermic peaks in c instead of the second exothermic peak in pure AP. The main exothermic peaks temperature of b (370 ℃) and c (380 ℃) is lower than that of pure AP (420 ℃), and the decomposition heat is 433 J/g for b and 298 J/g for c at 298 ℃.

Note: Appropriate safety precautions should be taken when preparing mixtures and it should be noticed that a total mass used is less than 1mg for all DSC runs.

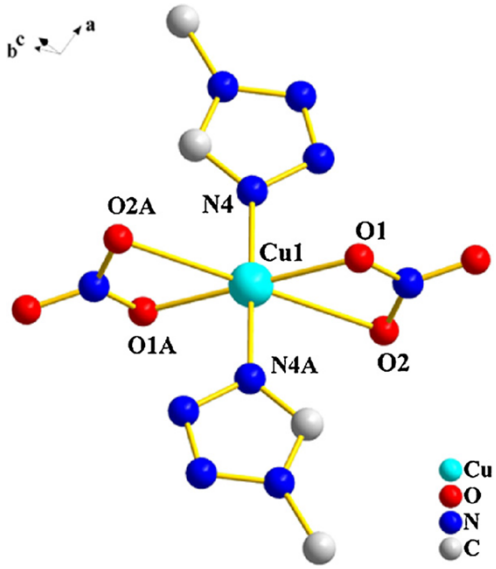

Fig. S10 Molecular unit and labeling scheme for compound $Cu(Mtta)_2(NO_3)_2$, H atoms were omitted for clarity.

In crystal of $Cu(Mtta)_2(NO_3)_2$, the coordination geometry around Cu(II) ion can be described as a distorted octahedron, of which the equatorial plan is defined by four oxygen atoms from two coordinated NO_3^- anions and the apical positions are occupied by two nitrogen atoms from two Mtta ligands.

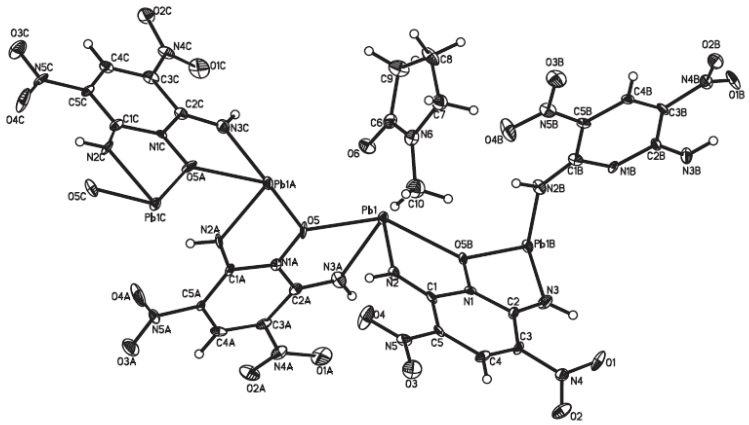

Fig. S11 Molecular structure of $[Pb_2(ANPyO)_2(NMP)\cdot NMP]_n$.

In the molecule of $[Pb_2(ANPyO)_2(NMP)\cdot NMP]_n$, NMP is N-Methyl pyrrolidone, each ligand ANPyO loses two protons ($C_5H_3N_5O_5^{2-}$) to coordinate with the central lead atom.

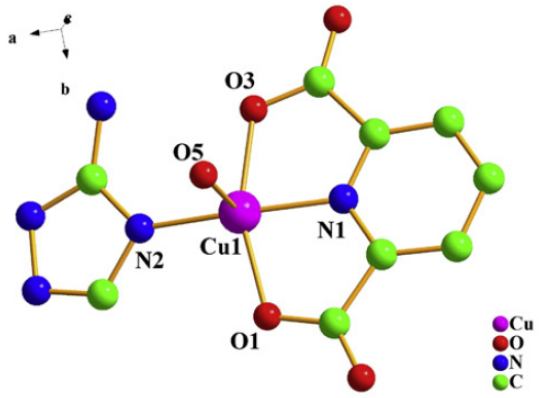

Fig. S12 Molecular structure of Cu(Hatrz)(pda)(H_2O)H_2O.

Compound Cu(Hatrz)(pda)(H_2O)H_2O has a zero-dimensional structural unit, Cu(II) ion is five-coordinated by two oxygen atoms and one nitrogen atom from one deprotonated pda ligand, one nitrogen atom from one Hatrz ligand and one oxygen atom from coordinated water molecule, forming a distorted square pyramidal coordination geometry.

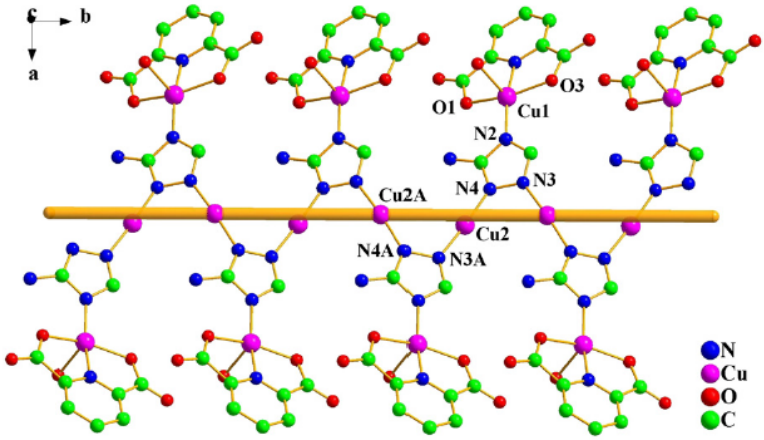

Fig. S13 1D mixed-valence helical chain along b-axis in Cu(I)Cu(II)(atrz)(pda)(H_2O).

Compound Cu(I)Cu(II)(atrz)(pda)(H_2O) exhibits a one-dimensional mixed-valence helical chain along b-axis, as seen from Fig. S13. Within the chain, there are two crystallographically independent Cu(I) and Cu(II) ions.

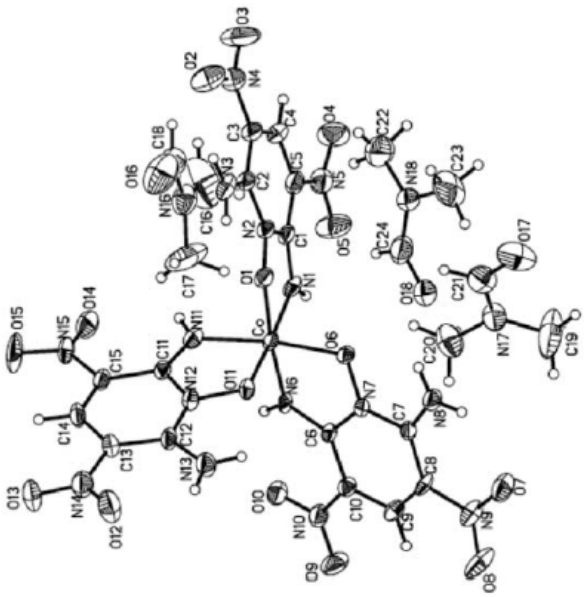

Fig. S14 Molecular structure of $[Co(ANPyO)_3]\cdot 3DMF$.

Each $[Co(ANPyO)_3]\cdot 3DMF$ comprises of one central iron cation and three deprotonated ANPyO anions as well as three lattice DMF molecules, joining to a six-coordinated structure through coordination bonds, electronic forces, and considerable hydrogen bonds. Each central iron atom has a distorted octahedron, coordinated by nitrogen and oxygen from deprotonated ANPyO.

Compounds $ZnAZT_6$ and $PbAZT_3$ are simple complexes of azotetrazole, they are synthesized and characterized as literature[31].